

Paramagnetic Instability at Normal-Metal – Superconductor Interfaces

Alban L. Fauchère^a, Wolfgang Belzig^b, and Gianni Blatter^a

^a*Theoretische Physik, Eidgenössische Technische Hochschule, CH-8093 Zürich, Switzerland*

^b*Institut für Theoretische Festkörperphysik, Universität Karlsruhe, D-76128 Karlsruhe, Germany*
(December 15, 1998)

We study the proximity coherence in a mesoscopic normal-metal film (N) in contact with a superconductor (S). Accounting for a repulsive interaction between the electrons in the normal metal, we find an enhanced local density of states close to the NS interface. The sharp peak in the density is pinned to the Fermi energy and leads to spontaneous paramagnetic interface currents. The induced orbital magnetic moments exhibit the characteristic features of paramagnetic reentrance observed in normal-metal coated superconducting cylinders [Phys. Rev. Lett. **65**, 1514 (1990)].

A normal metal in contact with a superconductor exhibits the phenomenon of proximity — the superconductor exports its coherent state across the interface into the normal metal. On a microscopic level, this phenomenon is described through the Andreev reflection of the normal-metal quasi-particles at the normal-metal–superconductor (NS) interface, converting normal- to supercurrent. Proximity superconductivity exhibits a rich phenomenology and has attracted considerable interest recently [1]. A particularly puzzling finding is the ultra-low-temperature reentrance observed in normal-metal coated superconducting cylinders [2], where, contrary to expectation, the fully diamagnetic cylinder develops a paramagnetic response at low temperatures. Recently, it has been speculated that a novel kind of persistent current states circling the cylinder might be responsible for this phenomenon [3], but closer inspection of the experimentally measurable quantities reveals that the predicted effect is too small [4]. In this Letter, we demonstrate that the presence of a repulsive electron-electron interaction in the normal metal naturally leads to the appearance of a paramagnetic instability at very low temperature, offering a possible explanation of the reentrance effect in the NS cylinders.

To be specific, we shall consider a clean normal-metal slab of thickness d ($0 < x < d$), in perfect contact with a bulk, conventional superconductor. The proximity effect is mediated by the Andreev reflection at the interface with the superconductor, which transforms incident electrons into back-reflected holes, thus binding the quasi-particles states to the normal layer for $E < \Delta_S$. In the usual free electron gas description of the normal metal, the Andreev bound states are found at $E_n = \hbar v_x(2n + 1)\pi/4d$ ($n = 0, 1, \dots$; $v_x = v_F \cos \vartheta$) producing a linear suppression of the DOS [5] $N(E) \sim N_0 E d / \hbar v_F$ close to the Fermi level $E = 0$ ($N_0 = m k_F / \hbar^2 \pi^2$). In the following we assume that the electron-electron interaction in the normal layer, which follows from the delicate balance between the phonon-mediated- and the Coulomb-interaction, is repulsive. As a consequence, a

finite order parameter $\Delta(x)$ is induced in the metal, opposite in sign as compared to Δ_S in the superconductor, see Ref. [6]. The NS junctions then behaves like a Josephson junction with a phase difference π , trapping quasi-particle states at the Fermi energy close to the NS interface. The local density of states $N(E, x)$ exhibits a peak at zero energy on top of the Andreev density of states, as shown in Fig. 1. This peak involves a macroscopic number of states with density $n_p \sim k_F^2/d$, which in the following we call the π -states.

The change in the DOS crucially affects the response of the proximity metal. The linear current response $j[A]$ can be divided into two contributions $j = j_{\text{dia}} + j_{\text{para}}$, the diamagnetic current $j_{\text{dia}} = -(e^2 n / mc) A$ giving the rigid response of the bulk density $n = k_F^3 / 3\pi^2$ and the paramagnetic current j_{para} following from the deformation of the wavefunction at the Fermi surface [7],

$$j_{\text{para}} = \frac{e^2 n}{mc} A \int dE \left(-\frac{\partial f}{\partial E} \right) \frac{N(E)}{N_0} \quad (1)$$

for slowly varying fields A (f is the Fermi occupation number). While in a bulk superconductor the paramagnetic current is quenched by the energy gap at low temperatures producing a net diamagnetic response, the paramagnetic current of a bulk normal metal cancels the diamagnetic current exactly. In the non-interacting metal under proximity, the linear density of states suppression $N(E) \propto E$ is still sufficient to suppress the paramagnetic current at zero temperature [8]. Including a repulsive interaction places the system in the opposite limit: The sharp DOS peak at the Fermi level produces a paramagnetic signal which *overcompensates* the diamagnetic response. Such a paramagnetic response naturally leads to an instability: The free energy $\delta F = -c j \delta A < 0$ can be lowered via a non-zero magnetic induction induced by spontaneous currents along the NS interface. The interface currents are associated with an orbital magnetization $M(T)$ producing a low-temperature reentrance in the magnetic susceptibility.

In the following we present a quantitative analysis

of the paramagnetic instability induced by the π -states. The magnetic induction $B_z(x)$ parallel to the surface is described by the vector potential $A_y(x)$ which drives the currents $j_y(x)$. The electron-electron interaction in the superconductor is accounted for by an effective coupling constant $V_S < 0$ and similarly $V_N > 0$ in the normal metal, see also Refs. [9,10]. Two self-consistency problems have to be solved: First, we evaluate the order parameter $\Delta(x)$ accounting for the different coupling constants in the superconductor and the normal metal, and obtain the local DOS $N(E, x)$. Second, we determine the current functional $j[A]$ which we solve together with Maxwell's equation to find the spontaneous interface currents.

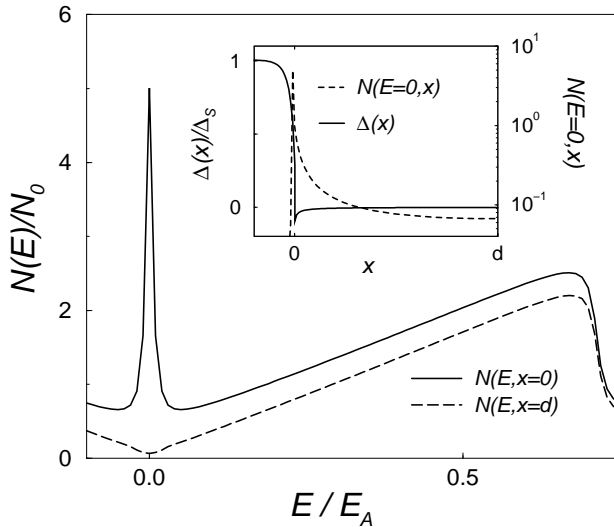


FIG. 1. Local DOS $N(E, x)$ at the NS interface $x = 0$ and at the metal boundary $x = d$ ($E_A = \hbar v_F/d$), as it follows from the self-consistent solution of the Eilenberger equation, Eqs. (2) and (3), for a thickness $d = 10\hbar v_F/\Delta_S$ and the coupling constants $V_S = -0.3$ and $V_N = 0.1$. Inset: Spatial dependence of the order parameter $\Delta(x)$ and local DOS $N(E = 0, x)$ at the peak energy (S: $x < 0$, N: $x > 0$).

We use the quasi-classical description following from the Eilenberger equation for \hat{g} ,

$$-\hbar v_x \partial_x \hat{g} = [\{\hbar\omega + iev_y A_y(x)/c\} \hat{\tau}_3 + \Delta(x) \hat{\tau}_1, \hat{g}], \quad (2)$$

where the 2×2 matrix \hat{g} contains the Green's functions $g_\omega(x, v_x)$ and $f_\omega(x, v_x)$ (ω Matsubara frequency, $v_x = v_F \cos \vartheta$, $\hat{\tau}_i$ Pauli matrices, see Ref. [11]). Eq. (2) is completed by the self-consistency relation for the pair potential ($\langle \dots \rangle$ is the angular average),

$$\Delta(x) = -V N_0 \pi T \sum_{\omega > 0} \langle f_\omega(x, v_x) \rangle. \quad (3)$$

The self-consistent numerical solution of Eqs. (2) and (3) is shown in the inset of Fig. 1. The course of the order parameter in the normal layer is asymptotically given by $\Delta(x) \sim -V_N N_0 \hbar v_F/x$, as expected from the f -function in the non-interacting case $V_N = 0$. $\Delta(x)$ decays

from a value $\sim -|V_N/V_S|\Delta_S$ at the NS interface, to $\sim -V_N N_0 \hbar v_F/d$ at the outer boundary. Close to the NS interface, the local DOS $N(E, x) = N_0 \text{Re}[\langle g_{-iE+\delta}(x, v_x) \rangle]$ exhibits a pronounced peak at zero energy, as shown in Fig. 1. In order to proceed with analytical results, we approximate the order parameter by a step function,

$$\Delta(x) = \begin{cases} \Delta_S, & x < 0, \\ -\Delta_N, & 0 < x < d, \end{cases}$$

where $\Delta_N \propto V_N$ enters as a parameter. The Green's function in the normal layer $x > 0$ can be determined exactly and takes the form

$$g_\omega(x, v_x) = \frac{\hbar\omega \sinh[\chi(d) - \gamma] + \Delta_N \cosh[\chi(d - x)]}{\hbar\Omega \cosh[\chi(d) - \gamma]}, \quad (4)$$

where $\chi(x) = 2\Omega x/v_x$, $\hbar^2\Omega^2 = \Delta_N^2 + \hbar^2\omega^2$, and $\tanh \gamma = \Delta_N/\hbar\Omega$ (we consider the limit $\Delta_S \gg \Delta_N, \hbar\omega$). The second term in (4) describes the π -states at the NS interface. The poles of the Green's function at $\hbar\omega = -iE + 0$ yield the bound state energies. While for $E \gg \Delta_N$ the Andreev states of the free electron gas are down-shifted by $\delta E_n \approx -2\Delta_N/(2n+1)\pi$ ($n = 0, 1, \dots$), below the gap $E < \Delta_N$ we find the π -states at

$$E = \Delta_N / \cosh \frac{2\sqrt{\Delta_N^2 - E^2}d}{\hbar v_x} \sim \Delta_N e^{-2\Delta_N d/\hbar v_x}, \quad (5)$$

exponentially close to Fermi energy. All trajectories with $v_x = v_F \cos \vartheta \ll \Delta_N d/\hbar$ possess a bound state at $E \approx 0$, thus producing the macroscopic weight of the zero energy DOS peak: For $\Delta_N > \hbar v_F/d$ the number of π -states per unit surface N_{surf} is equal to the number of transverse levels $N_{\text{surf}} \sim k_F^2$, while for $\Delta_N < \hbar v_F/d$ it is reduced to $N_{\text{surf}} \sim k_F^2 (\Delta_N d/\hbar v_F)^2$ via the reduction of the available solid angle $\cos \vartheta < \Delta_N d/\hbar v_F$.

We derive the current-field relations at low temperatures, assuming $k_B T \ll \hbar v_F/d, \Delta_N$. This implies a thermal length $\xi_N(T) = \hbar v_F/2\pi k_B T$ larger than the thickness d and no thermal smearing on the scale Δ_N . Only the trajectories with $\cos \vartheta < \Delta_N d/\hbar v_F$ contribute to the current at low temperatures. We describe them in the limit $\hbar v_x/\Delta_N d \rightarrow 0$ by

$$g_\omega(x, v_x) = \frac{\omega}{\Omega} + \frac{\omega \Delta_N}{\Omega (\hbar\Omega - \Delta_N)} e^{-\chi(x)}. \quad (6)$$

The current in the presence of a slowly varying vector potential A , follows from Eq. (6) after replacing ω by $\omega + iev_y A/\hbar c$ and inserting it into the current expression $j_y(x) = ieN_0 2\pi T \sum_{\omega > 0} \langle v_y g(x, v_x, v_y) \rangle$. In addition to the usual diamagnetic current $j_{\text{dia}} = -(c/4\pi\lambda^2) A$ [$\lambda = (mc^2/4\pi ne^2)^{-1/2}$ denotes the London length], we obtain the paramagnetic current

$$j_{\text{para}} \approx \frac{c}{4\pi\lambda^2} e^{-x/\alpha\xi_N^0} \alpha \frac{3\Phi_0}{2\pi\xi_N^0} \arctan \frac{ev_F A}{c\pi k_B T}, \quad (7)$$

in the limit $ev_F A/c, k_B T \ll \Delta_N$. Here, $\Phi_0 = \pi\hbar c/e$ denotes the flux quantum, $\xi_N^0 = \hbar v_F/2\Delta_N$ gives the extent of the π -states, and under the assumption $\Delta_N > \hbar v_F/d$ we have $\alpha = 1$. At temperatures $k_B T \gg ev_F A/c$ the paramagnetic current $j_{\text{para}} \sim (c/\lambda^2)(\Delta_N/k_B T)A$ is linear in A and $\propto 1/T$, a signature of the thermally smeared zero energy DOS peak, and competes with the diamagnetic current on the scale ξ_N^0 . At $T \rightarrow 0$, Eq. (7) is non-linear in the field and generates the spontaneous paramagnetic current. This paramagnetic interface current results from the energy splitting of the π -states in the field, $E \approx \pm ev_F A/c$, allowing the system to gain energy by shifting the DOS below the Fermi surface. For $\Delta_N < \hbar v_F/d$, the paramagnetic current is reduced by the factor $\alpha = (\Delta_N d/\hbar v_F) < 1$ in Eq. (7). The surface current $I = \int j dx \sim \alpha^2 c \Phi_0 / \lambda^2$ is in agreement with the current estimate $I_\pi \sim N_{\text{surf}} ev_F$ based on the number of π -states at zero energy. Eq. (7) thus always produces a net paramagnetic response at low temperature and fields.

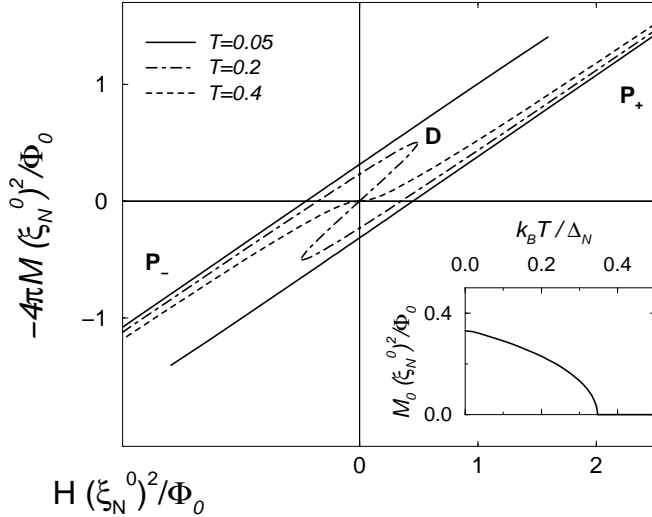


FIG. 2. Magnetization $M(T, H)$ curve at various temperatures (in units of Δ_N/k_B), for $\lambda = 0.3d$ and $\xi_N^0 = d$. The two meta-stable branches P_\pm exhibit a spontaneous magnetization in zero field, the diamagnetic branch D is unstable. Inset: Zero field magnetization $M_0(T)$.

The evaluation of the induced magnetization requires the self-consistent solution of Maxwell's equation $-\partial_x^2 A(x) = 4\pi j(x)/c$ together with the current functional $j[A(x)]$. The solution of the screening problem requires the full dispersive relation between $j(q)$ and $A(q)$, which in the proximity effect typically features a non-local current-field dependence on the scale ξ_N^0 [11]. Eq. (7) represents the long wavelength limit $q \rightarrow 0$. For simplicity, here we use Eq. (7) under the assumption of local response (accounting for the full non-locality does not af-

fect the qualitative nature of the final results, as we have checked numerically).

The magnetization curves $M(T, H)$, which follow from Eq. (7) are shown in Fig. 2. Approaching from large fields, Fig. 2 shows two paramagnetic branches P_\pm with a linear diamagnetic slope exhibiting a spontaneous magnetization in zero field. They result from the superposition of the paramagnetic magnetization $M_0(T)$ and the Meissner response to the applied field H . As the field is decreased (increased) past $H = 0$, the branch P_+ (P_-) becomes meta-stable. The spontaneous magnetization $M_0(T)$ appears below a second order transition point T_c^M and saturates at low temperatures, as shown in the inset of Fig. 2. The magnetization curve includes a diamagnetic branch D , which arises from the competition between the paramagnetic instability and the thermal smearing and is thermodynamically unstable.

In the following we give a semi-quantitative analysis of the magnetization $M = \int dx M(x)/d$, first at zero temperature and field $[M_0]$, proceeding to finite temperatures $[M_0(T)]$, and finally including an applied magnetic field H $[M(T, H)]$. The boundary conditions are given by $A(0) = 0$ and $\partial_x A(d) = H$. We concentrate on the most relevant limit where $\xi_N^0, d \gg \lambda$. At $T = 0$, according to Eq. (7), the paramagnetic interface current $j \sim \alpha c \Phi_0 / \lambda^2 \xi_N^0$ remains unscreened until being matched by $j_{\text{dia}} \sim -cA/\lambda^2$, producing a vector potential $A \sim \alpha \Phi_0 / \xi_N^0$ on the scale λ . The vector potential A saturates beyond λ , as the para- and diamagnetic currents cancel each other. Assuming that the π -states extend up to the outer metal surface ($\alpha < 1$), the induced magnetization $M = A(d)/4\pi d$ is given by

$$M_0 \sim \alpha \frac{\Phi_0}{\xi_N^0 d} \sim \frac{\Phi_0}{(\xi_N^0)^2}. \quad (8)$$

We note that although the spontaneous currents increase as $\Delta_N > \hbar v_F/d$ ($\alpha = 1$) they are screened exponentially beyond the extent of the π -states in this limit, giving a magnetization $M_0 \sim (\Phi_0/\xi_N^0 d) \exp[-(d - \xi_N^0)/\lambda]$. We assume $\alpha < 1$ in the following.

At finite temperature, the spontaneous magnetization is suppressed by the factor $\arctan(ev_F A/c\pi k_B T)$, which itself depends on the magnetization via $A \sim Md$, implying the implicit equation

$$\frac{M_0(T)}{M_0} \sim \arctan \frac{M_0(T)\alpha\Delta_N}{M_0 k_B T}. \quad (9)$$

The spontaneous magnetization appears below a second order transition at $k_B T_c^M \sim \alpha \Delta_N$, saturating at low temperatures, as shown in the inset of Fig. 2. The transition temperature is equal in magnitude to the energy splitting of the DOS peak $E \sim ev_F A/c \sim \alpha \Delta_N$.

Under an applied magnetic field H , the Meissner current j_{dia} screens both the spontaneous interface current and the applied field. At zero temperature we deal with

a linear problem and the magnetization is given by the superposition $M(H) = M_0 + \chi H$ of the spontaneous magnetic moment M_0 and the Meissner response χH . As the temperature increases, $M_0(T)$ decreases and the meta-stable regime shrinks. At $T > T_c^M$ the spontaneous magnetization in zero field has disappeared, the signature of the paramagnetic currents remains, however, reducing the diamagnetic susceptibility χ at small fields. At large temperature $T \gg T_c^M$ we recover the pure Meissner response.

Note that the two meta-stable branches P_+ and P_- in the magnetization curve, see Fig. 2, imply a first order transition with changing field at $H = 0$. The first order transition is similar to the magnetic breakdown occurring in the same system at large fields between the fully diamagnetic phase and a field penetration phase [12]. The rotation of the magnetic moments to the energetically more favorable polarization will show the hysteretic behavior typical for a first order transition. The transition from P_+ to P_- implies a paramagnetic slope in the thermodynamic dc -magnetization $\langle M(T, H) \rangle$, which will link the meta-stable solutions P_{\pm} in Fig. 2 and cross the origin at $M(H = 0) = 0$. In summary, we find that on approaching T_c^M from above, the diamagnetic susceptibility $\chi_{dc} = \langle M(T, H) \rangle / H$ is reduced, exhibiting a low-temperature reentrance. Below T_c^M , the spontaneous interface currents produce a net paramagnetic susceptibility χ_{dc} .

In the following we discuss our results in the context of the experiments by Mota and co-workers, who have measured the magnetic response of normal-metal coated superconducting cylinders at low temperatures [2,13]. Recent studies have established a quantitative understanding of the magnetic response of these samples at higher temperatures, explaining the sensitivity of the screening to small impurity concentration [11,14] due to the nonlocality and the magnetic breakdown at finite field [12]. The Nb-Ag and Nb-Cu cylinders show an anomalous paramagnetic signal in the magnetic response in the low-temperature – low-field corner of the $H - T$ phase diagram [2,15]. A direct comparison with our theory requires the magnetization curve $\langle M(T, H) \rangle$ which has not yet been measured. The observed dc -susceptibility $\chi_{dc}(T)$ as a function of temperature shows an increase at low temperature [16]. The measured ac -susceptibilities $\chi_{ac}(T)$ and $\chi_{ac}(H)$ exhibit a reentrance both as a function of temperature and field [2]. The reentrance is accompanied by an out-of-phase response signaling dissipation and by hysteresis in the field dependence. These features are in qualitative agreement with our results for the magnetization curve. We find that theory and experiment agree in order of magnitude for $\alpha^2 \sim 0.1$, implying a transition temperature $T_c^M \sim 100\text{mK}$ and a spontaneous magnetization $M_0 \sim 1\text{G}$. A more quantitative comparison with experiment requires a self-consistent treatment of the spontaneous currents with the pair potential, ac-

counting for the nonlocality of the current-field relation and its sensitivity to disorder.

In conclusion, we have demonstrated that the inclusion of a finite electron-electron repulsion in a proximity coupled normal-metal layer naturally produces spontaneous interface currents leading to a paramagnetic reentrance in the magnetic response: The sign change in the coupling across the NS interface leads to the trapping of π -states at the Fermi energy. The frustrated NS junction relaxes through the generation of spontaneous interface currents, inducing a paramagnetic moment. A non-trivial issue remains the requirement that the electron-electron interaction be repulsive at the low energy scales involved. Interesting consequences of this assumption have been discussed in the context of the proximity effect [6] and most recently in relation to the low temperature transport in mesoscopic NS structures [9,17]. In fact, the noble metal coatings used in the experiments of Mota and co-workers [2] appear to be the most plausible candidates for a repulsive electron-electron interaction. Turning the argument around, in the light of our findings the experimental observation of a paramagnetic reentrance can be taken as an indication of the presence of a repulsive interaction.

We acknowledge fruitful discussions with C. Bruder, M. Dodgson, V. Geshkenbein, C. Honerkamp, A. Mota, B. Müller, M. Rice, G. Schön, and M. Sigrist.

-
- [1] *Mesoscopic Electron Transport*, eds. L. P. Kouwenhoven *et al.*, NATO ASI Series E **345**, Kluwer Academic (1997).
 - [2] P. Visani, A. C. Mota, and A. Pollini, Phys. Rev. Lett. **65**, 1514 (1990).
 - [3] C. Bruder and Y. Imry, Phys. Rev. Lett. **80**, 5782 (1998).
 - [4] A. L. Fauchère, V. Geshkenbein, and G. Blatter, cond-mat/9809104.
 - [5] P. G. De Gennes and D. Saint-James, Phys. Lett. **4**, 151 (1963).
 - [6] P. G. De Gennes, Rev. Mod. Phys. **36**, 225 (1964).
 - [7] J. R. Schrieffer, *Theory of Superconductivity*, Addison-Wesley (1988).
 - [8] A. D. Zaikin, Solid State Commun. **41**, 533 (1982).
 - [9] Yu. V. Nazarov and T. H. Stoof, Phys. Rev. Lett. **76**, 823 (1996).
 - [10] F. Zhou, B. Spivak, and A. Zyuzin, Phys. Rev. B **52**, 4467 (1995).
 - [11] W. Belzig *et al.*, Phys. Rev. B **58**, 14531 (1998).
 - [12] A. L. Fauchère and G. Blatter, Phys. Rev. B **56**, 14102 (1997).
 - [13] A.C. Mota *et al.*, J. Low Temp. Phys. **76**, 465 (1989).
 - [14] F. B. Müller-Allinger *et al.*, cond-mat/980907.
 - [15] A.C. Mota *et al.*, Physica B **197**, 95 (1994).
 - [16] A. C. Mota *et al.*, in *Nanowires*, NATO ASI Series, Vol 340, 387-397 (1997).
 - [17] V. T. Petrashov *et al.*, Phys. Rev. Lett. **74**, 5268 (1995).